J. Biochem. 2017;162(1):17–25 doi:10.1093/jb/mvw102

JB THE JOURNAL OF BIOCHEMISTRY

PRMT2 interacts with splicing factors and regulates the alternative splicing of *BCL-X*

Received September 29, 2016; accepted December 11, 2016; published online January 17, 2017

Mynol I. Vhuiyan[1,‡], Magnolia L. Pak[1,†,‡], Margaret A. Park[2], Dylan Thomas[1,†], Ted M. Lakowski[3], Charles E. Chalfant[2,4,5] and Adam Frankel[1,*]

[1]Faculty of Pharmaceutical Sciences, The University of British Columbia, Vancouver, BC V6T 1Z3, Canada; [2]Department of Biochemistry and Molecular Biology, Virginia Commonwealth University, Richmond, VA 23298, USA; [3]College of Pharmacy, Pharmaceutical Analysis Laboratory, The University of Manitoba, Winnipeg, Manitoba R3E 0T5, Canada; [4]Hunter Holmes McGuire Veterans Administration Medical Center, Richmond, VA 23224, USA and [5]The Massey Cancer Center, Richmond, VA 23298, USA

*Adam Frankel, Faculty of Pharmaceutical Sciences, The University of British Columbia, Vancouver, British Columbia V6T 1Z3, Canada. Tel: +1-604-822-7146, Fax: +1-604-822-3035, email: afrankel@mail.ubc.ca

†Present addresses: Magnolia L. Pak, Department of Molecular, Cell and Cancer Biology, Howard Hughes Medical Institute, University of Massachusetts Medical School, Worcester, MA 01605, USA; Dylan Thomas, DynaLife$_{Dx}$, Edmonton, Alberta, Canada T5J 5E2; Department of Laboratory Medicine and Pathology, University of Alberta, Edmonton Alberta, T6G 2R3 Canada

‡These authors contributed equally to this work.

Protein arginine *N*-methyltransferase 2 (PRMT2) functions in JAK-STAT and Wnt/β-catenin signalling pathways, serves as a nuclear receptor-dependent transcriptional co-activator, and represses NF-κB and E2F1 transcription factor activities to promote apoptosis. We have previously demonstrated that PRMT2 interacts with PRMT1 and increases its activity. Here, we reveal associations using proteomics between the PRMT2 SH3 domain and splicing factors including Src-associated in mitosis 68 kDa protein (SAM68), a PRMT1 substrate and *trans*-acting factor that mediates *BCL-X* alternative splicing. We determined that PRMT2 interacts with SAM68 in cells and regulates its subcellular localization via the SH3 domain of PRMT2, prompting us to investigate the potential role of PRMT2 in *BCL-X* alternative splicing. We found that the expression of the full-length, wildtype form of PRMT2 promotes an increase in the *BCL-X(L)/BCL-X(s)* ratio in TNF-α or LPS stimulated cells. These results indicate that active PRMT2 may play a role during inflammation in alternative splicing regulation.

Keywords: alternative splicing; BCL-X; PRMT2; SAM68; SH3 domain.

Protein arginine *N*-methyltransferases (PRMTs) catalyse the transfer of methyl groups from *S*-adenosyl-L-methionine (AdoMet) to guanidino nitrogen atoms of arginine residues, yielding *S*-adenosyl-L-homocysteine (AdoHcy) and methylated arginine residues. Nine human PRMT family members have been discovered to date. PRMT1 (*1*), PRMT2 (*2*), PRMT3 (*3*), coactivator-associated arginine methyltransferase 1 (CARM1/PRMT4) (*4*, *5*), PRMT6 (*6*) and PRMT8 (*7*) form ω-N^G-monomethylarginine (MMA) and asymmetric ω-N^G,N^G-dimethylarginine (aDMA). PRMT5 (*8*) and PRMT9 (*9*) form MMA and symmetric ω-N^G,N'^G-dimethylarginine (sDMA), and PRMT7 only forms MMA (*10*, *11*). Several studies have uncovered PRMT roles in multiple cellular processes such as transcriptional regulation, signal transduction, RNA processing, DNA damage repair, cell cycle checkpoint, cell proliferation and differentiation (reviewed in (*12*)).

In contrast to other PRMT family members, the connection between PRMT2 enzymatic activity and its cellular functions remains somewhat enigmatic. Its comparatively weak enzymatic activity was initially observed when it was ectopically expressed as a green fluorescent protein fusion (*13*). Our group has shown that PRMT2 can methylate a glycine- and arginine-rich substrate and histone H4 *in vitro*, but its catalytic efficiency is orders of magnitude lower than that of PRMT1 (*2*), calling into question its relevance as an active enzyme. Although not directly demonstrated, PRMT2 has been implicated in the methylation of E1B-AP5 (hnRNP U-like 1) (*14*), histone H3 at Arg-8 (*15*) and STAT3 (*16*). Nevertheless, PRMT2-protein interactions rather than instances of substrate methylation have helped to define its roles. PRMT2 interacts with androgen and oestrogen receptors to serve as a transcriptional co-activator (*17*, *18*). PRMT2 can also form a transcriptionally repressive ternary complex with E2F and the retinoblastoma gene product that delays cell-cycle progression from G1 to S phase (*19*). PRMT2 can repress NF-κB activity by retaining a nuclear pool of IκB-α that prevents NF-κB-dependent transcription in cytokine-stimulated human and mouse embryonic fibroblast cell lines, as well as in LPS-stimulated lungs of mice (*20*, *21*). Our group has demonstrated that PRMT2 binds to and potentiates the activity of PRMT1 *in vitro* and in cells (*22*). The various protein complexes in which PRMT2 resides suggest that it participates in multiple cellular pathways.

PRMT2 contains uniquely among its family members an N-terminal Src homology 3 (SH3) domain, which is an ~60 amino acid protein-binding module conserved among signal transduction proteins such as the non-receptor tyrosine kinases Src and Abl that recognizes proline-rich motifs (*23*, *24*). The PRMT2 SH3

domain was shown in a protein-domain microarray to selectively bind proline-rich sequences in splicing factor SmB' and in SAM68 (*25*), and in another study it was required for the PRMT2 interaction with E1B-AP5 (*14*). Our own work has shown that the PRMT2 SH3 domain, although not directly involved in PRMT1 binding, does appear to regulate the interaction between PRMT1 and PRMT2 (*22*).

In order to gain insight into the biological functions of PRMT2, we identified proteins that associate with the PRMT2 SH3 domain using a proteomic approach. The majority of identified proteins were splicing-related factors, including the PRMT1 substrate SAM68 (*26*, *27*). We found that PRMT2 and SAM68 interact in HeLa cells, and ectopically expressed PRMT2 showed an SH3-domain dependent decrease in SAM68 co-localization in the nucleus in response to the methyltransferase inhibitor adenosine dialdehyde (AdOx). SAM68 is involved in the alternative splicing of the mitochondrial protein BCL-X to promote the small pro-apoptotic BCL-X(s) form of the protein over the large anti-apoptotic BCL-X(L) form (*28*). Likewise, we provide evidence in this study that PRMT2 is involved in regulating *BCL-X* alternative splicing in cells under inflammatory conditions.

Materials and Methods

DNA constructs

The glutathione-*S*-transferase (GST) gene (*Schistosoma japonicum*) was generated by inserting a stop codon at the 3′ end of the coding sequence in the pET41a(+) plasmid (Novagen) using the QuickChange site-directed mutagenesis (Agilent Technologies) and two complementary primers (5′-GTGGTGGCGA CCATCCTCCA TTAAAATCGG ATGGT TCAAC TAG-3′). The human SAM68 clone was purchased from ATCC (MGC-1286). SAM68 was PCR-amplified with primers (Forward: 5′-CGGAATTCAT GCAGCGCCGG GACGACCCC-3′; Reverse: 5′-AAGGAAAAAA GCGGCCGCTT AATAACGTCC ATA TGGGTG-3′) containing, respectively, *EcoRI* and *NotI* sites, and then inserted into the corresponding sites of pcDNA3.1 (*22*) to generate pcDNA3.1-HA-SAM68. The manufacture of vectors pcDNA3.1-HA-PRMT2, pcDNA3.1-HA-ΔSH3PRMT2, pcDNA3.1-PRMT2(E220Q), pcDNA3.1-mCitrine-PRMT1, pcDNA3.1-mCitrine-PRMT2 and pcDN A3.1-mCitrine-ΔSH3 was previously described (*22*). Bacterial expression vectors pGEX-2TK-SH3(Abl) and pGEX-2TK-SH3(PRMT2) were gifts from Dr Mark Bedford. Four pGFP-V-RS plasmid vectors and a control vector containing a scrambled sequence were acquired from OriGene. Each vector was designed to harbour a unique shRNA expression cassette targeting the 3′ untranslated region (3′UTR) of *PRMT2* mRNA.

Protein expression and purification

Recombinant proteins GST, GST-SH3(Abl), GST-SH3(PRMT2) and GST-PRMT2 were expressed in *Escherichia coli* and purified using previously described methods (*2*).

Proteomics

HeLa cells were harvested and lysed in hypotonic lysis buffer by repeated freezing and thawing as previously described (*22*). For the pull down assays, HeLa cell lysate (10 mg total protein) was incubated with 100 μg of GST, GST-SH3(Abl) or GST-SH3(PRMT2) in co-IP buffer (50 mM HEPES-KOH, pH 7.4, 150 mM NaCl, 1× protease inhibitor cocktail; Roche #04693132001) at 4 °C for 2 h with rotation. A volume of 50 μL of pre-washed glutathione (GSH)-sepharose (Genescript) was then added to each mixture. The GST pull-down experiments were carried out at 4 °C for 2 h with rotation in co-IP buffer with 0.1% (v/v) NP-40 (Sigma). The resin was washed five times with 1 ml of PBS (Gibco) containing 0.01% (v/v) NP-40. The bound proteins were eluted with 50 μL of 10 mM reduced GSH (Sigma) in 50 mM Tris−HCl (pH 8.0). Proteins from GST pull-down eluents were resolved on 10% SDS-PAGE gels and visualized by Colloidal Coomassie Blue stain. Six gel slices from the GST-SH3(PRMT2) pull-down lane and a gel slice from an empty lane were digested with trypsin, and desalted using ZipTip (Millipore) C-18 cartridges. Tryptic fragments were analysed using an API QSTAR PULSARI Hybrid LC−MS/MS and identified by a human database search using the MASCOT (Matrix Science) search engine. Five missed trypsin cleavages were allowed for the database search. Carboxymethylation, N-terminal acetylation, deamidation and mono- and dimethylation (Arg) were included in the search as possible modifications. The peptide mass tolerance allowed in the matching process was ± 1.2 Da, and the fragment mass tolerance was set at ± 0.5 Da. Peptide sequence matches considered insignificant (P 0.05) based on MASCOT scoring or found in the negative control were eliminated from the list of hits.

Tissue culture

HeLa and HEK293T cells were cultured in Dulbecco's Modified Eagle's Medium (DMEM) (Sigma) supplemented with 10% foetal bovine serum (FBS) (Gibco), 50 units/ml penicillin and 50 μg/ml streptomycin (Gibco) (standard growth medium) at 37 °C in 5% CO_2. For transfections, ~0.6×10^6 HeLa cells were seeded in a six-well plate containing standard growth medium 1 day prior to transfection. The growth medium was initially replaced with Opti-MEM medium (Invitrogen), and cells were transfected with 4.0 μg of DNA using 8.0 μL of Lipofectamine 2000 (Invitrogen) per the manufacturer's instructions. The Opti-MEM medium was replaced with the standard growth medium (DMEM supplemented with 10% FBS, 50 units/ml penicillin and 50 μg/ml streptomycin). The transfected cells were cultured for an additional 16 h before they were harvested.

For *PRMT2* knock down by siRNA, HEK293T cells at ~30% confluence were transfected with 50 nM of PRMT2-specific siRNA-A (Invitrogen, 10620310), siRNA-B (Sigma, PDSIRNA2D), or scramble RNA (Santa Cruz, sc-37007) as a control using Opti-MEM and Lipofectamine RNAiMAX (Invitrogen) according to the manufacturer's instructions. Opti-MEM was replaced with the standard growth medium 8 h post-transfection, and cells harvested after 48 h.

For transfections with shRNA constructs, the standard growth medium for HEK293T cells was replaced with Opti-MEM medium (Invitrogen), and the cells were transfected with 2.5 μg of DNA using 5.0 μL of Lipofectamine 3000 (Invitrogen) per the manufacturer's instructions. The medium was replaced with standard growth medium containing puromycin (3 μg/ml) 24-h post-transfection. The transfected cells were passaged every 3–4 days and monitored by IncuCyte Zoom live cell imaging system (Essen Bioscience) for GFP positive cells to confirm puromycin selection. For rescue experiments in these cells, transfection of DNA proceeded as described above. The Opti-MEM medium was replaced with the standard growth medium 24-h post-transfection. The cells were then treated with either TNF-α (100 ng/ml) (BD Pharmingen) or LPS (1 μg/ml) (Sigma-Aldrich) for 24 h before they were harvested.

Co-immunoprecipitations

Anti-HA antibody (H3663, Sigma) or mouse IgG (Sigma) was cross-linked to the NHS-activated sepharose (GE Healthcare) per manufacturer's instructions. The cross-linked resin was pre-blocked in 3% (w/v) BSA in PBS at 4 °C for 1 h. Cell lysates were incubated with 50 μL pre-blocked anti-HA- or mouse IgG-cross-linked sepharose in 250 μL co-IP buffer at 4 °C for 2 h. Subsequently, the resin was washed thoroughly with 0.05% (v/v) Tween 20 in PBS (Gibco) five times before bound proteins were eluted in SDS-PAGE sample buffer.

Western blotting

Proteins were separated on 10% SDS-PAGE gels, transferred to nitrocellulose or PVDF membranes, and blotted with anti-ADMA (39231, Active Motif), anti-SAM68 (sc-333, Santa Cruz), anti-PRMT2 (sc-135010, Santa Cruz), or anti-HA (H3663, Sigma) antibodies. Goat anti-mouse IgG-HRP (sc-2005) or goat anti-rabbit IgG-HRP (sc-2054, Santa Cruz) and ECL Western blotting detection reagents (GE Healthcare) were used for protein visualization.

Immunofluorescence and confocal microscopy

Approximately 1.0×10^7 HeLa cells were transiently transfected with 24 μg pcDNA3.1-mCitrine-PRMT1, pcDNA3.1-mCitrine-PRMT2 or pcDNA3.1-mCitrine-ΔSH3PRMT2 using 48 μL of Lipofectamine 2000 (Invitrogen) per the manufacturer's instructions. The Opti-MEM medium was replaced with standard growth medium 8 h post-transfection. The transfected cells were split 24 h post-transfection and re-seeded onto a 12-mm microscope cover glass (Fisher) coated with poly-D-lysine (Sigma) in a 24-well plate in standard growth medium. To inhibit cellular methylation, 20 μM AdOx was added to the media. The cells were then allowed to grow to 80% confluence before fixation with a 4% paraformaldehyde solution in PBS.

The cell membrane was permeabilized by incubating the cells in 0.1% (v/v) Triton X-100 in PBS at room temperature for 5 min, followed by three 5-min washes with PBS. To block non-specific binding of the antibody, the cells were incubated in 1% BSA (w/v) in PBS at room temperature for 30 min. The cells were first blotted with an anti-SAM68 antibody at 1:50 dilution, then with an Alexa Fluor 546-conjugated goat anti-rabbit secondary antibody (Invitrogen) at a 1:1,000 dilution, both in 1% BSA (w/v) in PBS with 0.1% Tween-20 (v/v) (PBST) at room temperature for 1 h with three 5-min washes between each step. Subsequently, the cells were stained with 50 nM DAPI at room temperature for 10 min before they were washed and mounted on microscope slides (Fisher). Cell images were captured at ambient temperature using an Olympus FluoView FV10i confocal microscope at 60× magnification with an oil lens, and were processed with ImageJ software (NIH image).

Total RNA extraction and qRT-PCR

Total RNA was extracted from HEK293T cells using Trizol reagent (Life Technologies) following the manufacturer's instructions. RNA was resuspended in DEPC-treated water (Life Technologies) and stored at −80 °C. Reverse transcriptase reactions were performed using 2.0 μg of total RNA and SuperScript VILO mastermix (Life Technologies) per manufacturer's instructions. For evaluation of *PRMT2* and *BCL-X* splice variant expression levels, cDNA was subjected to qPCR using Life Technologies TaqMan primer/probe sets for *PRMT2* (Assay Hs00181759_m1), *PRMT2ΔSH3* (Assay Hs00895400_m1), *BCL-X(L)* (Assay Hs00236329_m1), *BCL-X(s)* (forward primer 5′-GAG CTT TGA ACA GGA TAC T-3′; reverse primer 5′-ACC AGC GGT TGA AGC GTT-3′; probe 5′-6-FAM GCA GCC GAG AGC CGA AAG GG MGB-NFQ-3′) and *GAPDH* (Assay Hs99999905_m1) and TaqMan Universal PCR Master Mix (Life Technologies). Samples were analysed using a StepOnePlus real-time PCR system (Applied Biosystems). Transcript levels were calculated using the standard curve method and were normalized to GAPDH for corresponding samples.

Results

Identification of PRMT2 SH3 domain-associated proteins

To identify potential PRMT2-protein interactions mediated through the PRMT2 SH3 domain, we performed a GST pull-down assay using GST fused to the N-terminal SH3 domain of PRMT2 (GST-SH3(PRMT2)) as bait and total protein from HeLa cell lysate as prey (Fig. 1). GST and GST fused to the SH3 domain of the Abl tyrosine kinase (GST-SH3(Abl)) were included as negative and positive controls, respectively. As shown in Fig. 1, proteins bound to GST-SH3(PRMT2) and GST-SH3(Abl) showed comparable protein banding patterns, implying that both SH3 domains recognize a similar array of ligands. However, at least six bands were enriched in the GST-SH3(PRMT2) pull down in comparison to the other two samples.

Proteins in the six bands from the GST-SH3(PRMT2) pull down lane (Fig. 1) were identified by LC – MS/MS following tryptic digest. All thirty-seven hits (Table I) were identified by at least two matched peptides with ion scores above the significance threshold. The majority of hits are reported to participate in pre-mRNA processing and contain proline-rich motifs. Proteomic analysis also revealed new as well as known sites of arginine methylation. A western blot of the GST pull-down samples with an anti-ADMA antibody provides additional evidence that the SH3 domain of PRMT2 associates with methylated proteins to a greater extent than GST-SH3(Abl) and GST alone (Fig. 1).

PRMT2 associates with SAM68 in cells

We investigated the interaction between PRMT2 and the identified hit SAM68. The *in vitro* association of SAM68 with the PRMT2 SH3 domain was confirmed in a GST pull-down assay by western blot analysis (Fig. 2A). Despite this interaction, we did not detect PRMT2 activity toward SAM68 in methylation assays analysed by phosphorimaging or mass spectrometry

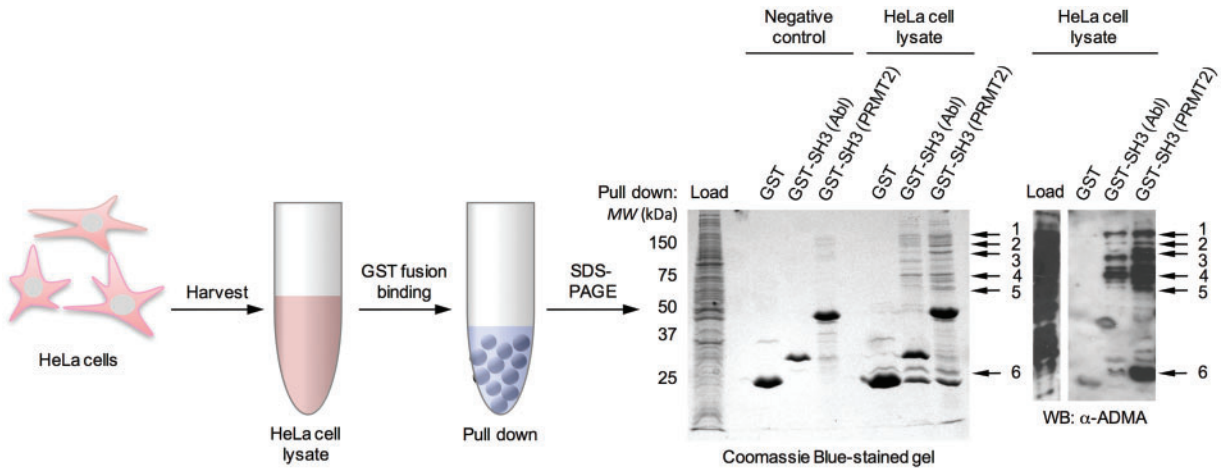

Fig. 1 Identification of PRMT2 SH3 domain-associated proteins. HeLa cell lysates were prepared for GST pull-down experiments. Samples were separated by gel electrophoresis, and protein bands 1 – 6 were isolated from the Coomassie Blue-stained gel for proteomic analysis. GST pull-down samples were also probed for methylated proteins by the western blot using an anti-ADMA antibody.

Table I. Identified proteins that associate with the SH3 domain of PRMT2 from gel slices

Gene name	Protein name	Gel slice(s)	Arginine methylation[c]
Sm core snRNP components			
SNRPB	Small nuclear ribonucleoprotein-associated proteins B and B′	6	***
U1 snRNP components			
SNRNP70	U1 small nuclear ribonucleoprotein 70 kDa	3 – 5	–
U2 snRNP components			
DDX42	ATP-dependent RNA helicase DDX42	1	–
SF3A1	Splicing factor 3A subunit 1	1	–
SF3A2	Splicing factor 3A subunit 2	3, 4	*
SF3A3	Splicing factor 3A subunit 3	4, 5	–
SF3B3	Splicing factor 3B subunit 3	1	–
SNRPB2	U2 small nuclear ribonucleoprotein B''	6	–
USP39	U4/U6.U5 tri-snRNP-associated protein 2	4	–
U11/U12 snRNP components			
PDCD7	Programmed cell death protein 7	5	–
hnRNPs			
FUS	Heterogeneous nuclear ribonucleoprotein P2	3, 5	***
HNRNPK	Heterogeneous nuclear ribonucleoprotein K	4	**
HNRNPL	Heterogeneous nuclear ribonucleoprotein L	4	*
HNRNPR	Heterogeneous nuclear ribonucleoprotein R	3	**
HNRNPU	Heterogeneous nuclear ribonucleoprotein U	1	**
Other splicing-related proteins			
HNRNPUL1	Heterogeneous nuclear ribonucleoprotein U-like protein 1	1	**
HSPA1A	Heat shock 70 kDa protein 1A/1B	3	–
HSPA8	Heat shock cognate 71 kDa protein	3	–
HSPB1	Heat shock protein beta-1	6	–
KHDRBS1	Src-associated in mitosis 68 kDa protein	3	**
LUC7L3[a]	Luc7-like protein 3	5	–
NONO	Non-POU domain-containing octamer-binding protein	5	–
PSPC1	Paraspeckle component 1	4	*
PUF60	60 kDa poly(U)-binding-splicing factor	4	–
RBM25	RNA-binding protein 25	1	–
RBM39[a]	RNA-binding protein 39	3	–
SF1	Splicing factor 1	2, 3	–
SFPQ	Splicing factor, proline- and glutamine-rich	1, 2	***
WBP11	WW domain-binding protein 11	2	–
Cleavage and polyadenylation proteins			
CPSF5	Cleavage and polyadenylation specificity factor subunit 5	6	*
CPSF6	Cleavage and polyadenylation specificity factor subunit 6	3 – 5	–
CPSF7	Cleavage and polyadenylation specificity factor subunit 7	5	–
Other proteins			
CCT3	T-complex protein 1 subunit gamma	4	–
CCT4	T-complex protein 1 subunit delta	5	–
CCT7	T-complex protein 1 subunit eta	5	–
PRMT2[b]	Protein arginine *N*-methyltransferase 2	1 – 6	–
WASL	Neural Wiskott-Aldrich syndrome protein	3	–
WIPF1	WAS/WASL-interacting protein family member 1	5	*

The PRMT2 SH3 domain binders identified in the six protein bands analysed by LC–MS/MS are listed. See Supplementary Table SI for accession numbers, scores, sequence coverage, and the total number of non-redundant peptides.
[a]Protein does not contain any proline-rich sequence.
[b]Identified peptides were from the SH3 domain.
[c]Sequence details for sites of arginine methylation can be found in Supplementary Table SII.
*Novel sites of arginine methylation identified in this proteomic study.
**Human proteins annotated as arginine methylated in the Uniprot database but not identified in our proteomic study.
***Human proteins annotated as arginine methylated in both the Uniprot database and in our proteomic study.

(data not shown). We then tested to see if PRMT2 could also interact with SAM68 in HeLa cell lysate by co-IP. Endogenous PRMT2 associated with hemagglutinin (HA)-tagged SAM68 (Fig. 2B), and in a reciprocal experiment HA-PRMT2 enriched for endogenous SAM68 above the IgG control (Fig. 2C). No association was detected between HA-ΔSH3PRMT2 and endogenous SAM68 (Fig. 2D).

Richard *et al*. previously showed that AdOx at a 1.0-mM concentration caused some SAM68 to accumulate in the cytoplasm (*26*). We wanted to test if PRMT2 can affect the subcellular localization of SAM68 in response to AdOx. We transfected HeLa cells with vectors coding for the fluorescent protein mCitrine fused to PRMT1, PRMT2, or ΔSH3-truncated PRMT2, and visualized endogenous SAM68 by immunostaining. HeLa cells cultured in the presence of 20 μM AdOx did not elicit any change in the nuclear localization of SAM68 (Fig. 3A). A similar result was obtained for cells expressing mCitrine-PRMT1, which co-localized with SAM68 to the nucleus (Supplementary data, Fig. S1). However, we did observe some disruption of

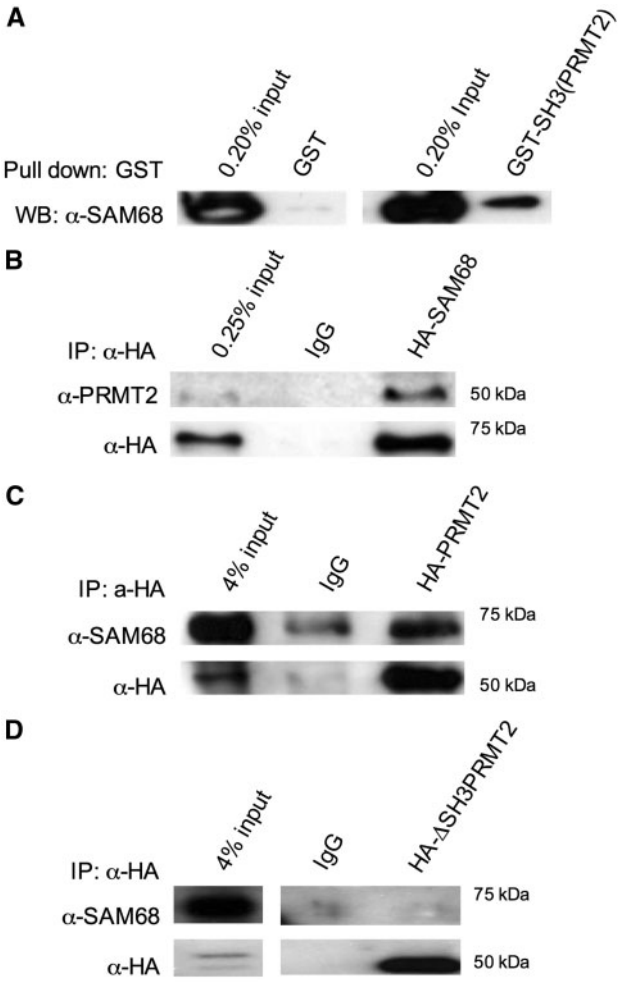

Fig. 2 The interaction between SAM68 and PRMT2 is dependent on the PRMT2 SH3 domain. (**A**) Proteins bound to GST pull-downs from HeLa cell lysate were resolved by gel electrophoresis and blotted with an anti-SAM68 antibody. Whole cell lysate from HeLa cells that expressed HA-SAM68 (**B**), HA-PRMT2 (**C**), or HA-ΔSH3PRMT2 (**D**) were immunoprecipitated with anti-HA or mouse IgG (negative control) and blotted as indicated.

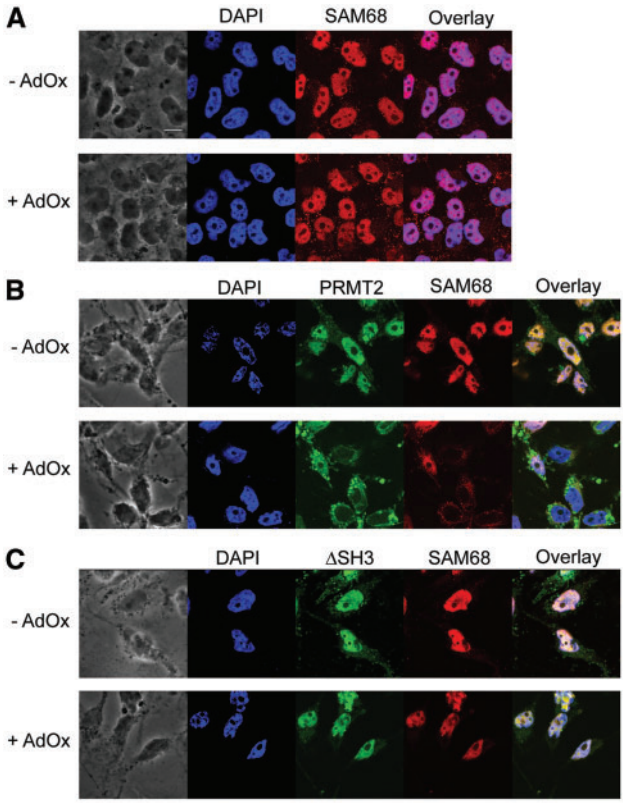

Fig. 3 PRMT2 affects the subcellular localization of SAM68. HeLa cells untransfected (**A**) or transfected with mCitrine-PRMT2 (**B**, *green*) or mCitrine-ΔSH3 (**C**, *green*) were treated with or without 20 μM AdOx as indicated. SAM68 was immunostained with anti-SAM68 and Alexa Fluor 546-conjugated antibodies (*red*). Nuclei were visualized by DAPI stain (*blue*). The phase contrasted images (*left*) and the merged images (*right*) are also shown. The scale bar indicates 10 μm.

nuclear co-localization of SAM68 and mCitrine-PRMT2 upon AdOx treatment (Fig. 3B; see Supplementary data, Fig. S2 for a larger field of view). This effect did not occur when the truncated form of PRMT2 (mCitrine-ΔSH3) was expressed (Fig. 3C), indicating that the localization of SAM68 is dependent on PRMT2 bearing its SH3 domain.

PRMT2 influences the alternative splicing of BCL-X

The interaction between PRMT2 and SAM68 prompted us to investigate whether PRMT2 can also influence alternative splicing of the *BCL-X* transcript. We carried out siRNA-mediated knockdown experiments of *PRMT2* expression in HEK293T cells. By qRT-PCR, we found that *PRMT2* transcript levels were reduced by 4.6- and 3.8-fold for siRNA-A and siRNA-B, respectively, compared to the scramble siRNA control (Fig. 4A). These reductions in *PRMT2* expression resulted in slightly lowered *BCL-X(L)*/*BCL-X(s)* ratios (Fig. 4B) while total *BCL-X* transcript levels did not decrease (Supplementary data, Fig. S3A). Additionally, we transfected HEK293T cells with shRNAs targeting the 3′-untranslated region of *PRMT2* mRNA, and assessed *PRMT2* transcript expression by qRT-PCR. The greatest decrease in *PRMT2* expression (48% lower than control) occurred with shRNA-A (Fig. 4C). Despite this decrease, we found that shRNA-A did not significantly alter the *BCL-X(L)*/*BCL-X(s)* ratio in this experiment (Fig. 4D).

Since *BCL-X* is a target gene for NF-κB (*29*, *30*), we activated the NF-κB pathway by treating HEK293T cells with TNF-α or LPS to observe changes to *BCL-X* alternative splicing attributable to different *PRMT2* levels under inflammatory conditions. Both TNF-α and LPS treatments caused significant increases in the *BCL-X(L)*/*BCL-X(s)* ratio in shRNA control groups, but these increases were reduced by 20% and 30%, respectively, in cells harbouring shRNA-A (Fig. 4F) where *PRMT2* expression levels were modestly reduced (Fig. 4E). The reduction in *BCL-X(L)*/*BCL-X(s)* ratios were not accompanied by decreases in total *BCL-X* transcript levels (Supplementary data, Fig. S3B). These results indicate that *PRMT2* levels influence the alternative splicing of *BCL-X* in response to inflammation.

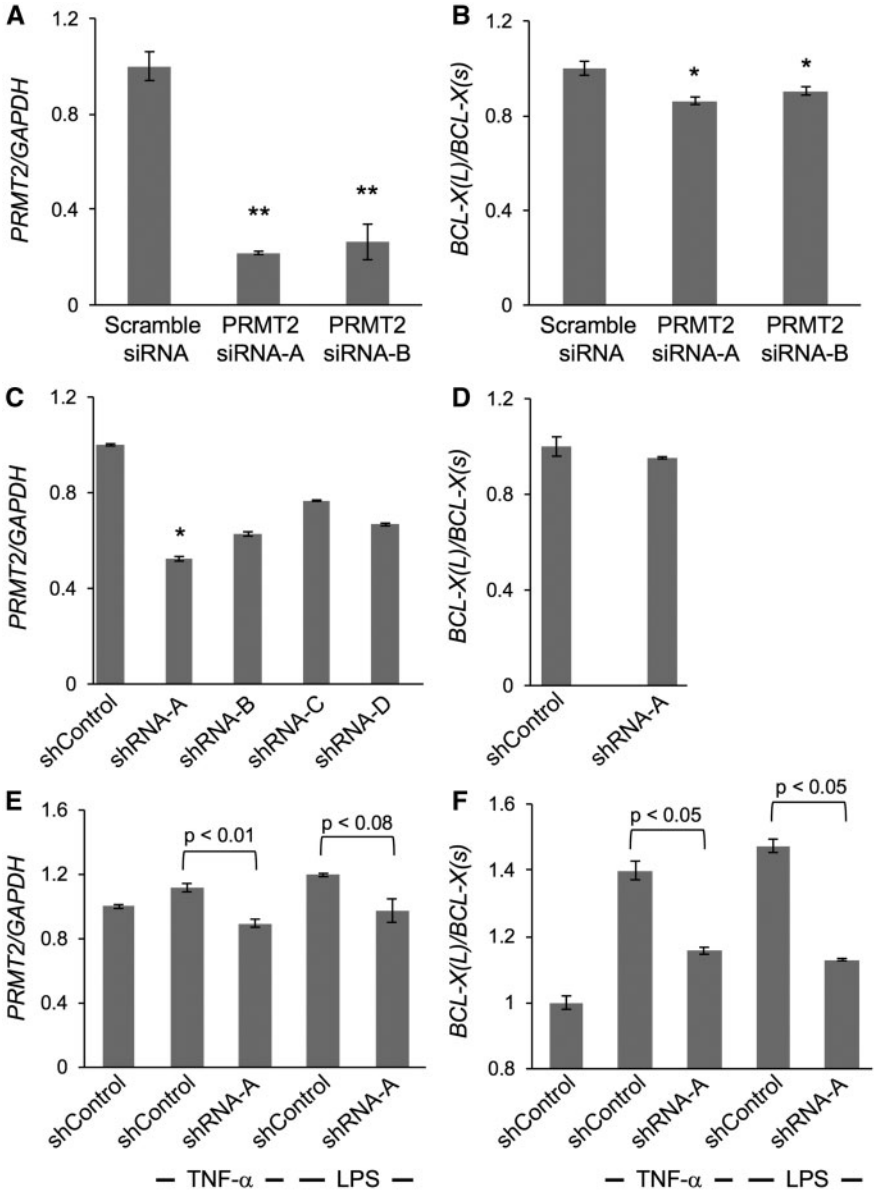

Fig. 4 The effect of *PRMT2* expression levels on *BCL-X* alternative splicing under inflammatory conditions. HEK293T cells transfected with scramble RNA or PRMT2-targeted siRNAs were harvested 48 h post-transfection and qRT-PCR was performed to show *PRMT2*/*GAPDH* (**A**), and the relative amounts of *BCL-X* transcript ratios normalized to the scramble siRNA control (**B**). HEK293T cells were transfected with control shRNA (shControl) or PRMT2-targeted shRNAs, and harvested for qRT-PCR to show *PRMT2* normalized to *GAPDH* (**C**). The relative amounts of *BCL-X* transcript ratios for shRNA-A and shControl treated cells were determined by qRT-PCR and normalized to the shControl samples (**D**). HEK293T cells harbouring shControl or shRNA-A were treated with either TNF-α or LPS and harvested after 24 h of treatment. qRT-PCR was performed to show *PRMT2* normalized to *GAPDH* (**E**), and *BCL-X* transcript ratios (**F**). Standard deviations of two replicates are shown. Statistical comparisons between experimental samples were analysed using a Student's *t*-test (*$P<0.05$; **$P<0.005$).

We then tested to see if the observed decrease in the *BCL-X(L)/BCL-X(s)* ratio can be reversed by PRMT2 overexpression. In a series of rescue experiments, we transfected shRNA-containing HEK293T cells with a mammalian expression vector for HA-PRMT2, HA-ΔSH3PRMT2, the catalytically inactive HA-PRMT2(E220Q) (*22*), or the vector-only control (pcDNA3.1) prior to treating cells with either TNF-α or LPS. As anticipated, high expression levels of *PRMT2* caused significant increases in the *BCL-X(L)/BCL-X(s)* ratio, whereas the ratio remained unchanged with high expression levels of truncated or inactive forms of PRMT2 (Fig. 5). Taken together, these data indicate that full-length, catalytically active PRMT2 promotes the formation of *BCL-X(L)* over *BCL-X(s)*.

Discussion

PRMT2 SH3 domain selectivity

In this study, we used the SH3 domain of PRMT2 as a molecular handle to identify potential PRMT2 binding partners. Several high-resolution SH3 domain structures reveal a well-conserved overall topology that consists of two perpendicular β sheets formed by five or six antiparallel β strands (*31*). Similar to other

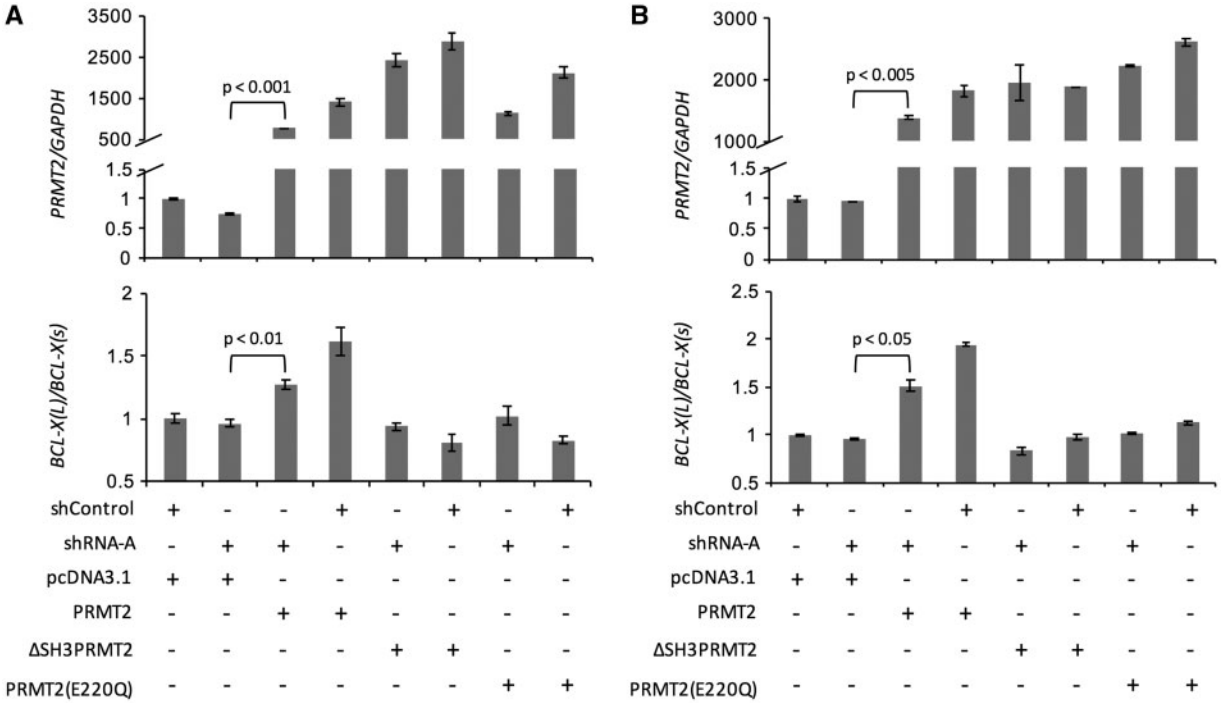

Fig. 5 The effect of added *PRMT2* on *BCL-X* alternative splicing under inflammatory conditions. HEK293T cells harbouring shControl or shRNA-A targeting PRMT2 were transfected with pcDNA3.1 (negative control), or plasmids encoding HA-PRMT2, HA-ΔSH3PRMT2, or HA-PRMT2(E220Q). After 24 h of transfection, cells were treated with TNF-α or LPS and harvested after 24 h of treatment. qRT-PCR was performed to show *PRMT2* normalized to *GAPDH*, and *BCL-X* transcript ratios for TNF-α (**A**) or LPS (**B**) treatment groups. Standard deviations of two replicates are shown. Statistical comparisons between experimental samples were analysed using a Student's *t*-test.

proteins like Src and Abl, the ligand binding surface on the PRMT2 SH3 domain consists of two shallow, hydrophobic grooves and one acidic groove that could readily complement ligands bearing either the class I target sequence (R/K)xxPxxP or the class II target sequence xPxxPx(R/K). Typically, these ligands exhibit affinities for SH3 domains within the K_D range of 1−200 μM. Despite the weak to modest affinities of these interactions, they contribute to binding where selectivity can be achieved through subcellular compartmentalization of binding partners and/or formation of multi-protein complexes (*32*). Since all but two of the proteins found to associate with the PRMT2 SH3 domain contain one or more proline-rich sequence stretches, it is probable that the large majority of identified proteins act as direct ligands.

PRMT involvement in pre-mRNA splicing

Richard *et al*. showed early on that an anti-sDMA-specific antibody or hypomethylated nuclear extracts could inhibit splicing reactions (*33*), implicating type II activity in splicing events. It is well established that the methylation of spliceosomal Sm proteins by PRMT5 is required so that the survival motor neuron (SMN) protein can facilitate the assembly of snRNPs (*34–36*). Recently, the type II enzyme PRMT9 was shown to methylate splicing factor 3B subunit 2 (SF3B2) as an important step in U2 snRNP maturation for efficient splicing (*9*). Examples of type I enzyme involvement in splicing have also come to light. Yu *et al*. used a genome-wide ChIP-chip analysis to reveal the involvement of the yeast homologue of PRMT1, Hmt1, in the co-transcriptional recruitment of pre-mRNA splicing factors to intron-containing genes (*37*). Similarly, CARM1's methylation of splicing factors CA150, SF3B4, SmB and U1C extends its activity from transcriptional co-activation to splicing (*38*). PRMT6 also exhibits a dual role as both an oestrogen-dependent transcriptional co-activator and a mediator of exon skipping (*39*).

Studies have demonstrated a role for PRMT2 and its truncated splice variants as transcriptional co-activators (*17*, *18*, *40*, *41*), but the involvement of PRMT2 in pre-mRNA processing has yet to be explored. In this work, we have identified associations between the PRMT2 SH3 domain and many splicing-related proteins, which include the Sm core snRNP protein SmB/B', components of both major and minor snRNPs, splicing regulators such as hnRNPs, and other splicing-related proteins (Table I). Twelve of these proteins contain at least one dimethylated arginine residue, including the CARM1 substrate SmB (*38*) and five novel substrates. The weak enzymatic activity of PRMT2 may preclude it from being directly responsible for methylating these substrates, but its ability to act as a scaffold through its SH3 domain suggests a role in mediating interactions. Indeed, we have previously demonstrated using co-IP and biomolecular fluorescence complementation that PRMT1 and PRMT2 interact in HeLa cells to produce a heteromeric complex (*22*). In this study, the SH3 domain of PRMT2 appears to play an important role in its interaction with SAM68 as demonstrated in co-localization experiments.

The association of PRMT2 with SAM68 and other splicing-related proteins led us to explore a role for PRMT2 in pre-mRNA processing. It has been demonstrated that SAM68 together with hnRNP A1 promotes the formation of small pro-apoptotic *BCL-X(s)* over large anti-apoptotic *BCL-X(L)* via 5′ alternative splice site selection, and this effect was reversed upon tyrosine phosphorylation of SAM68 by the Src-like kinase Fyn (*28*). RBM25 and Luc7L3, also known to promote *BCL-X(s)* transcript formation (*42*), are two other proteins identified by mass spectrometry in our study to associate with the PRMT2 SH3 domain. SF3B1, a component of the U2 snRNP complex for which several other components have been identified to associate with the PRMT2 SH3 domain (Table I), promotes formation of BCL-X(L) over BCL-X(s) (*43*). Our results demonstrating that PRMT2 promotes *BCL-X(L)* formation suggests that PRMT2 antagonizes SAM68, RBM25, and Luc7L3 functions in *BCL-X* alternative splicing.

PRMT2's effect on *BCL-X* alternative splicing became apparent only when cells were treated with either TNF-α or LPS, indicating that cell stress from inflammatory mediators may set up conditions for PRMT2 to act. Inflammatory stresses activate the NF-κB pathway, culminating in the expression of a large number of target genes including *BCL-X* (*29*, *30*). The induction of the NF-κB-mediated stress response and *de novo* expression of *BCL-X* in this instance may factor into what is required for PRMT2 to contribute to the alternative splicing of *BCL-X*. Our results also indicate that full-length and catalytically active PRMT2 promotes formation of the larger *BCL-X* transcript, indicating that its interactions and substrate methylation are needed to affect splicing. The mechanism by which PRMT2 participates in this process, and whether PRMT2 is capable of impacting the splicing of other transcripts will help to shed light on the role PRMT2 plays in post-transcriptional processing.

Supplementary Data

Supplementary Data are available at *JB* Online.

Acknowledgements

We thank Dr Leonard Foster and Mrs. Suzanne Perry at the Centre for High Throughput Biology at UBC for advice on proteomic experiments, and Dr. Mark Bedford at the University of Texas M.D. Anderson Cancer Center for generously donating GST fusion expression vectors for Abl and PRMT2 SH3 domains.

Funding

This work was supported by The Natural Sciences and Engineering Research Council of Canada RGPIN-2015-04450 (A.F.) and RGPIN-2015-06543 (T.M.L), the BC Proteomics Network (A.F.), the Dr Paul H.T. Thorlakson Foundation Fund (T.M.L), University of Manitoba Research Grants Program (T.M.L), the Veteran's Administration Merit Award BX001792, a National Institutes of Health Research Career Scientist Award via HL072925 and CA154314, and the US-Israel Binational Science Foundation via BSF#2011380 (C.E.C). D.T. and M.I.V were supported by Four-year University Graduate Fellowship Awards from The University of British Columbia.

Conflict of Interest

None declared.

References

1. Lin, W.J., Gary, J.D., Yang, M.C., Clarke, S., and Herschman, H.R. (1996) The mammalian immediate-early TIS21 protein and the leukemia-associated BTG1 protein interact with a protein-arginine N-methyltransferase. *J. Biol. Chem.* **271**, 15034–15044
2. Lakowski, T.M., and Frankel, A. (2009) Kinetic analysis of human protein arginine N-methyltransferase 2: formation of monomethyl- and asymmetric dimethyl-arginine residues on histone H4. *Biochem. J.* **421**, 253–261
3. Tang, J., Gary, J.D., Clarke, S., and Herschman, H.R. (1998) PRMT 3, a type I protein arginine N-methyltransferase that differs from PRMT1 in its oligomerization, subcellular localization, substrate specificity, and regulation. *J. Biol. Chem.* **273**, 16935–16945
4. Chen, D., Ma, H., Hong, H., Koh, S.S., Huang, S.M., Schurter, B.T., Aswad, D.W., and Stallcup, M.R. (1999) Regulation of transcription by a protein methyltransferase. *Science* **284**, 2174–2177.
5. Schurter, B.T., Koh, S.S., Chen, D., Bunick, G.J., Harp, J.M., Hanson, B.L., Henschen-Edman, A., Mackay, D.R., Stallcup, M.R., and Aswad, D.W. (2001) Methylation of histone H3 by coactivator-associated arginine methyltransferase 1. *Biochemistry* **40**, 5747–5756.
6. Frankel, A., Yadav, N., Lee, J., Branscombe, T.L., Clarke, S., and Bedford, M.T. (2002) The novel human protein arginine N-methyltransferase PRMT6 is a nuclear enzyme displaying unique substrate specificity. *J. Biol. Chem.* **277**, 3537–3543
7. Lee, J., Sayegh, J., Daniel, J., Clarke, S., and Bedford, M.T. (2005) PRMT8, a new membrane-bound tissue-specific member of the protein arginine methyltransferase family. *J. Biol. Chem.* **280**, 32890–32896
8. Branscombe, T.L., Frankel, A., Lee, J.H., Cook, J.R., Yang, Z., Pestka, S., and Clarke, S. (2001) PRMT5 (Janus kinase-binding protein 1) catalyzes the formation of symmetric dimethylarginine residues in proteins. *J. Biol. Chem.* **276**, 32971–32976
9. Yang, Y., Hadjikyriacou, A., Xia, Z., Gayatri, S., Kim, D., Zurita-Lopez, C., Kelly, R., Guo, A., Li, W., Clarke, S. G., and Bedford, M.T. (2015) PRMT9 is a type II methyltransferase that methylates the splicing factor SAP145. *Nat. Commun.* **6**, 6428
10. Miranda, T.B., Miranda, M., Frankel, A., and Clarke, S. (2004) PRMT7 is a member of the protein arginine methyltransferase family with a distinct substrate specificity. *J. Biol. Chem.* **279**, 22902–22907
11. Zurita-Lopez, C.I., Sandberg, T., Kelly, R., and Clarke, S.G. (2012) Human protein arginine methyltransferase 7 (PRMT7) is a type III enzyme forming ω-NG-monomethylated arginine residues. *J. Biol. Chem.* **287**, 7859–7870
12. Bedford, M.T., and Clarke, S.G. (2009) Protein arginine methylation in mammals: who, what, and why. *Mol. Cell.* **33**, 1–13
13. Herrmann, F., Pably, P., Eckerich, C., Bedford, M.T., and Fackelmayer, F.O. (2009) Human protein arginine methyltransferases in vivo–distinct properties of eight canonical members of the PRMT family. *J. Cell Sci.* **122**, 667–677
14. Kzhyshkowska, J., Schütt, H., Liss, M., Kremmer, E., Stauber, R., Wolf, H., and Dobner, T. (2001)

Heterogeneous nuclear ribonucleoprotein E1B-AP5 is methylated in its Arg-Gly-Gly (RGG) box and interacts with human arginine methyltransferase HRMT1L1. *Biochem. J.* **358**, 305–314

15. Blythe, S.A., Cha, S.W., Tadjuidje, E., Heasman, J., and Klein, P.S. (2010) beta-Catenin primes organizer gene expression by recruiting a histone H3 arginine 8 methyltransferase, Prmt2. *Dev. Cell.* **19**, 220–231
16. Iwasaki, H., Kovacic, J.C., Olive, M., Beers, J.K., Yoshimoto, T., Crook, M.F., Tonelli, L.H., and Nabel, E.G. (2010) Disruption of protein arginine N-methyltransferase 2 regulates leptin signaling and produces leanness in vivo through loss of STAT3 methylation. *Circ. Res.* **107**, 992–1001
17. Qi, C., Chang, J., Zhu, Y., Yeldandi, A.V., Rao, S.M., and Zhu, Y.J. (2002) Identification of protein arginine methyltransferase 2 as a coactivator for estrogen receptor alpha. *J. Biol. Chem.* **277**, 28624–28630
18. Meyer, R., Wolf, S.S., and Obendorf, M. (2007) PRMT2, a member of the protein arginine methyltransferase family, is a coactivator of the androgen receptor. *J. Steroid Biochem. Mol. Biol.* **107**, 1–14
19. Yoshimoto, T., Boehm, M., Olive, M., Crook, M.F., San, H., Langenickel, T., and Nabel, E.G. (2006) The arginine methyltransferase PRMT2 binds RB and regulates E2F function. *Exp. Cell Res.* **312**, 2040–2053
20. Ganesh, L., Yoshimoto, T., Moorthy, N.C., Akahata, W., Boehm, M., Nabel, E.G., and Nabel, G.J. (2006) Protein methyltransferase 2 inhibits NF-kappaB function and promotes apoptosis. *Mol. Cell. Biol.* **26**, 3864–3874
21. Dalloneau, E., Pereira, P.L., Brault, V., Nabel, E.G., and Hérault, Y. (2011) Prmt2 regulates the lipopolysaccharide-induced responses in lungs and macrophages. *J. Immunol.* **187**, 4826–4834
22. Pak, M.L., Lakowski, T.M., Thomas, D., Vhuiyan, M.I., Hüsecken, K., and Frankel, A. (2011) A protein arginine N-methyltransferase 1 (PRMT1) and 2 heteromeric interaction increases PRMT1 enzymatic activity. *Biochemistry* **50**, 8226–8240
23. Pawson, T., and Gish, G.D. (1992) SH2 and SH3 domains: from structure to function. *Cell* **71**, 359–362
24. Ren, R., Mayer, B.J., Cicchetti, P., and Baltimore, D. (1993) Identification of a ten-amino acid proline-rich SH3 binding site. *Science* **259**, 1157–1161
25. Espejo, A., Côté, J., Bednarek, A., Richard, S., and Bedford, M.T. (2002) A protein-domain microarray identifies novel protein-protein interactions. *Biochem. J.* **367**, 697–702
26. Côté, J., Boisvert, F.M., Boulanger, M.C., Bedford, M.T., and Richard, S. (2003) Sam68 RNA binding protein is an in vivo substrate for protein arginine N-methyltransferase 1. *Mol. Biol. Cell.* **14**, 274–287
27. Bedford, M.T., Frankel, A., Yaffe, M.B., Clarke, S., Leder, P., and Richard, S. (2000) Arginine methylation inhibits the binding of proline-rich ligands to Src homology 3, but not WW, domains. *J. Biol. Chem.* **275**, 16030–16036
28. Paronetto, M.P., Achsel, T., Massiello, A., Chalfant, C.E., and Sette, C. (2007) The RNA-binding protein Sam68 modulates the alternative splicing of Bcl-x. *J. Cell Biol.* **176**, 929–939
29. Barkett, M., and Gilmore, T.D. (1999) Control of apoptosis by Rel/NF-kappaB transcription factors. *Oncogene* **18**, 6910–6924
30. Pahl, H.L. (1999) Activators and target genes of Rel/NF-kappaB transcription factors. *Oncogene* **18**, 6853–6866
31. Cohen, G.B., Ren, R., and Baltimore, D. (1995) Modular binding domains in signal transduction proteins. *Cell* **80**, 237–248
32. Mayer, B.J. (2001) SH3 domains: complexity in moderation. *J. Cell Sci.* **114**, 1253–1263
33. Boisvert, F.M., Côté, J., Boulanger, M.-C., Cléroux, P., Bachand, F., Autexier, C., and Richard, S. (2002) Symmetrical dimethylarginine methylation is required for the localization of SMN in Cajal bodies and pre-mRNA splicing. *J. Cell Biol.* **159**, 957–969
34. Friesen, W.J., Paushkin, S., Wyce, A., Massenet, S., Pesiridis, G.S., Van Duyne, G., Rappsilber, J., Mann, M., and Dreyfuss, G. (2001) The methylosome, a 20S complex containing JBP1 and pICln, produces dimethylarginine-modified Sm proteins. *Mol. Cell. Biol.* **21**, 8289–8300
35. Meister, G., Eggert, C., Bühler, D., Brahms, H., Kambach, C., and Fischer, U. (2001) Methylation of Sm proteins by a complex containing PRMT5 and the putative U snRNP assembly factor pICln. *Curr. Biol.* **11**, 1990–1994
36. Meister, G., and Fischer, U. (2002) Assisted RNP assembly: SMN and PRMT5 complexes cooperate in the formation of spliceosomal UsnRNPs. *EMBO J.* **21**, 5853–5863
37. Chen, Y.-C., Milliman, E.J., Goulet, I., Côté, J., Jackson, C.A., Vollbracht, J.A., and Yu, M.C. (2010) Protein arginine methylation facilitates cotranscriptional recruitment of pre-mRNA splicing factors. *Mol. Cell. Biol.* **30**, 5245–5256
38. Cheng, D., Côté, J., Shaaban, S., and Bedford, M.T. (2007) The arginine methyltransferase CARM1 regulates the coupling of transcription and mRNA processing. *Mol. Cell.* **25**, 71–83
39. Harrison, M.J., Tang, Y.H., and Dowhan, D.H. (2010) Protein arginine methyltransferase 6 regulates multiple aspects of gene expression. *Nucleic Acids Res.* **38**, 2201–2216
40. Zhong, J., Cao, R.-X., Hong, T., Yang, J., Zu, X.-Y., Xiao, X.-H., Liu, J.-H., and Wen, G.-B. (2011) Identification and expression analysis of a novel transcript of the human PRMT2 gene resulted from alternative polyadenylation in breast cancer. *Gene* **487**, 1–9.
41. Zhong, J., Cao, R.-X., Zu, X.-Y., Hong, T., Yang, J., Liu, L., Xiao, X.-H., Ding, W.-J., Zhao, Q., Liu, J.-H., and Wen, G.-B. (2012) Identification and characterization of novel spliced variants of PRMT2 in breast carcinoma. *FEBS J.* **279**, 316–335
42. Zhou, A., Ou, A.C., Cho, A., Benz, E.J., and Huang, S.C. (2008) Novel splicing factor RBM25 modulates Bcl-x pre-mRNA 5' splice site selection. *Mol. Cell. Biol.* **28**, 5924–5936
43. Massiello, A., Roesser, J.R., and Chalfant, C.E. (2006) SAP155 Binds to ceramide-responsive RNA cis-element 1 and regulates the alternative 5' splice site selection of Bcl-x pre-mRNA. *FASEB J.* **20**, 1680–1682